THE JOURNAL OF PHYSICAL CHEMISTRY B

ARTICLE

pubs.acs.org/JPCB

Length Scales Necessary for Proper Averaging to Characterize Polymerization in Nanosystems: Topochemical Polymerization of Diacetylene Nanocrystals Dispersed in a Polystyrene Matrix As Probed by Confocal Raman Microscopy

Yu Nemoto and Masahito Sano*

Department of Polymer Science and Engineering, Yamagata University, 4-3-16 Jyonan, Yonezawa, Yamagata 992-8510, Japan

ABSTRACT: The scales necessary to make appropriate spatial averaging on solid-state polymerization were investigated by confocal Raman microscopy with a mapping resolution of 2 μm. Nanocrystals of an aliphatic diacetylene with an average size of 0.14 μm, each separated by 0.3 μm on average, were dispersed in a polystyrene matrix and were polymerized by UV irradiation. The distribution of nanocrystals was inhomogeneous over approximately 20 μm scale. A large crystal of the same monomer shows that photoinitiation is already averaged at the microscope resolution, while the color transition from the blue to the red form requires a scale greater than 5 μm. For the nanocrystals at low conversion, UV−vis absorption spectroscopy measured over a centimeter scale indicates linear polymerization kinetics and a higher polymer yield at a higher temperature. By contrast, the Raman microscopy reveals that, whereas the 20 μm region of high monomer concentrations yields more polymers at −24 °C, the region of low monomer concentrations gives more polymers at 20 °C. We propose thermal initiation, which is not efficient in the large crystals, as an additional initiation process for the apparent discrepancy, implying that the initiation process is not averaged below 20 μm scale for the dispersed nanocrystals.

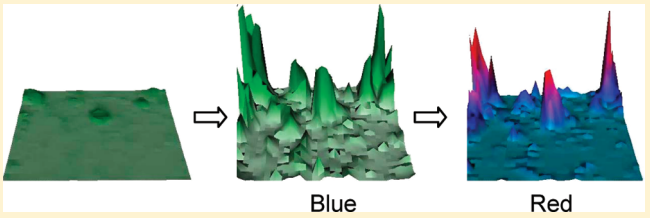

1. INTRODUCTION

Our present formalism on polymerization kinetics is based on spatial averaging over proper scales. In solution under ordinary reaction conditions, molecules collide repeatedly before diffusing apart and may react at one of the collisions. Then, the effect of decreased mobility due to rapidly increasing viscosity can be neglected to a large extent by taking spatial averages longer than the diffusing distance.[1] In this way, the coordinate at which the molecule has reacted has no meaning to the next reaction, and only the average distance between molecules becomes relevant. As a result, spatial dependence is hidden within concentration dependence and does not appear in kinetics explicitly. A similar situation is realized in the case of large solid crystals. Although each molecule is fixed at a particular coordinate, there are many equivalent molecules with the same relative positions in each crystalline domain. Because polymerization is initiated at many points within a domain and most chains grow independent of their coordinates, averaging over the domain takes away the spatial part of kinetics. In contrast, for molecules confined in nanosized solutions or solids, such averaging may no longer be effective. For instance, a nanocrystal can accommodate only a few initiation sites, and the crystal size is comparable to the growing polymer chain. Additionally, the crystal surface that occupies an increasingly large fraction as the crystal size becomes smaller may have significant influence on the chain growth. Thus, many polymerization characteristics are not averaged within a nanocrystal, or equivalently, polymerization in each nanocrystal proceeds differently. This implies that there must be a transition point on the scale or the number of nanocrystals at which the whole system becomes describable by averaged values, rather than specifying the individual set of properties observed at each nanocrystal. It becomes important to discuss, given an ensemble of differently polymerizing nanocrystals, what scales or how many nanocrystals are necessary to make averaging meaningful. Obviously, averaging over a macroscopic scale that contains Avogadro's number of nanocrystals will clear it, whereas several nanometers that include only a few nanocrystals may not be enough. The former, however, may "over-average" and conceal relevant variations possibly existing in the nano systems. With the radius of gyration of a typical polymer being on the order of a few tens of nanometers, a micrometer scale is a conceivable scale in order that polymerization properties are properly averaged while unveiling local differences. In this study, we are interested in possible variations on the polymerization of nanocrystals averaged over a micrometer scale. These variations, in turn, guide us to understand the polymerization characteristics of nanocrystals.

Confocal Raman microscopy (CRM) is a powerful tool to analyze three-dimensional (3D) distribution of each chemical species without damaging the sample. A laser is focused at a particular coordinate within a sample. CRM has an aperture in

Received: August 25, 2011
Revised: October 3, 2011
Published: October 05, 2011

dx.doi.org/10.1021/jp208238d | *J. Phys. Chem. B* 2011, 115, 12744–12750

front of the spectrometer so that only a reflected light from the focal plane is allowed to pass through. Analyzing Raman scattered light gives a vibrational spectrum containing all Raman active species present at the focal plane. By scanning the focus over the sample volume and acquiring a Raman spectrum at each coordinate, 3D distribution of each component can be mapped. Since the Raman process involves vibration of induced dipole moments, a substance with finite absorption at the laser wavelength shows enhancement of the scattered intensity. With the visible laser wavelength, a colored sample can be detected even at a nanosized amount. Being an optical device, its resolution is limited by diffraction. Under typical experimental conditions of imaging organic compounds in air, it is an order of 1 μm. Thus, CRM is not capable of resolving species within a nanocrystal. It is, however, able to differentiate nanocrystals separated by a few micrometers, which is a situation easily producible by crystallization in a polymer matrix.

Diacetylene compounds are known to undergo solid-state polymerization from monomer crystal to polymer crystal, initiated by γ-ray radiation, UV light, and thermal treatment. Due to their topochemical nature, only those monomers whose lattice parameters agree with those of the polymer within several percent can polymerize. In macroscopic systems, polymerization reaction is governed almost solely by crystalline structures.[2] Strain produced by an accumulated lattice mismatch between the monomer and the polymer induces stress on the crystal as polymerization continues. The aliphatic diacetylene monomer we used in this study is colorless. Upon UV irradiation, diradicals are formed and propagate as butatriene.[3] Termination reactions stabilize the chain in the acetylene structure, giving a blue color to the crystal. Further irradiation causes the color to change again to red. The so-called blue form represents polymer in a high crystalline order. The red color is believed to originate from distortion of the extended π-system, mostly caused by crystalline disorder in the alkyl chains.[4,5]

In this study, spatial dependence of topochemical polymerization of diacetylene nanocrystals was followed. The nanocrystals were made by crystallizing monomer within a cosolidifying thin polystyrene (PS) film. Instability during solvent evaporation caused inhomogeneous distributions of monomer nanocrystals. The size and separation of nanocrystals were adjusted so that they were much smaller than the CRM resolution and inhomogeneity, but comprised discrete units for the polymerization reaction. Polymerization was initiated by UV light at various temperatures, and the subsequent growth of polymer was mapped at the same fixed location. The result demonstrates that the scale for proper spatial averaging depends on each process governing the reaction.

2. EXPERIMENTAL SECTION

2.1. Materials. Pentacosa-10,12-diynoic acid (PCDA) (Wako Pure Chemical Ind.), atactic PS (M_w = 125 000−250 000, PolyScience, Inc.), and all other solvents were used as received.

Large crystals (on the order of 0.1 mm) of PCDA were grown in either *N*,*N*-dimethylformamide or dimethyl sulfoxide solutions by slow evaporation of solvents. No difference was observed between these solvents. To grow nanocrystals, equal amounts of 0.1 wt % toluene solution of PCDA and 1.0 wt % toluene solution of PS were mixed thoroughly. A drop of the mixture was spread on a glass or Teflon plate, and the solvent was allowed to evaporate over a few days at room temperature in a dark room. The resulting solid film was clear and colorless, and was a few hundred micrometers thick.

Both large crystals and PCDA nanocrystals in PS were polymerized by irradiating unpolarized UV light (254 nm, 950 μW/cm^2 at 15 cm away), after equilibrating at a controlled temperature in the dark. To ensure uniform irradiation, the light source was held about 5 cm above the film and moved constantly as if drawing a hemisphere over the sample. The substrate plate had a marker on its surface so that CRM mapping could be performed at the same position each time after it was taken out from the microscope stage.

2.2. Characterization. Polymerization was followed by UV−vis absorption spectroscopy (Jasco V-570) with light passing through an area of around 1 cm^2. Atomic force microscopy (AFM, NanoScope IV) was used to measure the size distribution of PCDA nanocrystals. In order to image, the nanocrystals in the PS film were irradiated by UV light for several hours until the sample turned red. The film was dissolved in toluene, and the mixture was centrifuged at 15000*g* for 15 min. The supernatant was removed, and fresh toluene was added. This process was repeated several times to remove PS. The final dispersion was cast on mica and dried before being imaged by AFM.

Small-angle X-ray diffraction (SAXRD, Rigaku NANO-Viewer) and wide-angle X-ray diffraction (WAXRD, Rigaku MicroMax007) were measured using Cu Kα line at room temperature. The PS film containing nanocrystals was pealed from the substrate and cut into small pieces. These pieces were collected and randomly packed for measurements. The same piece (1.4 mg) was used for differential scanning calorimetry (DSC, Seiko Instrument DSC 6220) with a heating rate of 3 °C/min.

2.3. Confocal Raman Microscopy. CRM (Nicolet Almega XR) was operated with 780 nm laser excitation with a 50x dry objective (N.A. = 0.75) and an aperture of 50 μm, typically. Although the diffraction limited spot size and depth were calculated to be 0.6 and 3 μm, respectively, refraction in air and the film broadened them.[6] By mapping the interfacial region, we estimated the diameter of the focused laser beam and the actual depth resolution to be approximately 1 and 10 μm, respectively. The laser beam was focused below the film surface and scanned horizontally with a step of either 2.0 or 5.0 μm. Thus, the obtained Raman image represented a chemical map of an ∼10 μm thick section sliced horizontally, with a mapping resolution slightly larger than the optical resolution.

3. RESULTS AND DISCUSSION

3.1. Raman Spectroscopy. Figure 1 shows Raman spectra of the nanocrystal in PS as the monomer, the blue form polymer at low conversion, and the red form polymer. A large crystal gave similar spectra but with some differences as described below. The colored polymer phases give much stronger Raman scattering than the colorless monomer due to finite absorption at 780 nm. We also tried 532 nm excitation for stronger resonance effects, but faced the problem that the laser irradiation induced polymerization.

The large crystal exhibits a sharp peak at 2250, 2080, and 2120 cm^{-1} in each spectrum, respectively, all of which are assigned as the ν_1 (C≡C stretch) mode based on the previous Raman studies.[7−12] Although the ν_2 (C═C stretch) and ν_3 (C═C bend) appearing around 1490 and 1200 cm^{-1} are also available to produce Raman maps, the intensities of the ν_1 peaks are employed in the present study because they are free of PS peaks appearing in 500−1600 cm^{-1} in the nanocrystal samples.

Whereas the monomer ν_1 in the nanocrystals appeared at the same position as in the large crystal, the blue form ν_1 in the nanocrystals was upshifted by several cm^{-1} from the large crystal peak, depending on the measured sample. A previous study has shown that the ν_1 mode is highly sensitive to strain on the polymer chain and its upshift corresponds to smaller tensile strain.[12] This means that polymer chains are strained less in the nanocrystals than in the large crystal. Apparently, monomer molecules in the nanocrystals are able to reorient easier in order to release strain on the polymer chain. The magnitude of upshifting depends on the sample. For large crystals, the tensile strain is related to conversion. If a similar relation holds for the nanocrystals, the varying magnitude indicates that the crystal quality determined when they have been formed in a PS matrix has a large influence on the reaction. This is an expected result for topochemical polymerization.

3.2. Raman Mapping of Large Crystals. Figure 2 exhibits Raman maps of the blue and red forms, as well as their optical microscopic images. The monomer large crystal gave a very low signal-to-noise (S/N) ratio under the same experimental conditions as the polymer crystals. We did not scan further since increasing the laser intensity induced polymerization of the monomer. Figure 2a represents an intensity distribution of the blue form at an early stage of polymerization at room temperature. A uniform distribution indicates that polymerization appears to proceed uniformly over the whole crystal, as seen with the mapping resolution of 2 μm.

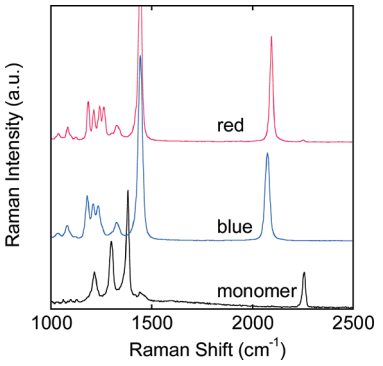

Figure 1. Raman spectra of the PCDA nanocrystals in PS as the monomer, the blue form polymer, and the red form polymer.

As the polymerization continues, the blue form is gradually transformed to the red form. At the same time, the crystal is broken apart into pieces of around 5 μm with major cracks running along the *b*-axis (parallel to the polymer chain), due to crystalline stress developed by the accumulated lattice mismatch. Figure 2c, showing an intensity ratio of the red to blue forms, reveals the higher red form ratio toward the right in this particular crystal, but nearly uniform distribution within each broken piece. The rightward intensity variation is accidental, probably caused by intrinsic accumulation of stronger stress on one side during crystal growth and handling. CRM indicates that the color transition has progressed uniformly within each broken crystal, but has occurred randomly over broken pieces.

3.3. Size and Distribution of Nanocrystals in PS. The size and number of nanocrystals in a PS matrix are important parameters for both CRM mapping and polymerization reaction. Figure 3 shows the statistics of AFM image heights of tetragonal nanocrystals. The histogram can be deconvoluted to two curves of a tailing function (the χ^2 function is used tentatively, although the exact functional form is not relevant) with peaks at nearly doubling positions. Because some nanocrystals are likely to have aggregated during the PS removal process, a tailing part and the second curve are interpreted as secondary aggregates. Then, the size of primary particles distributes in 0.05−0.2 μm, and the first peak at 0.14 μm may be taken as the average nanocrystal size. From the initial loading amount of PCDA, the number of nanocrystals in 1.0 μm^3 PS film is estimated to be around 30, which

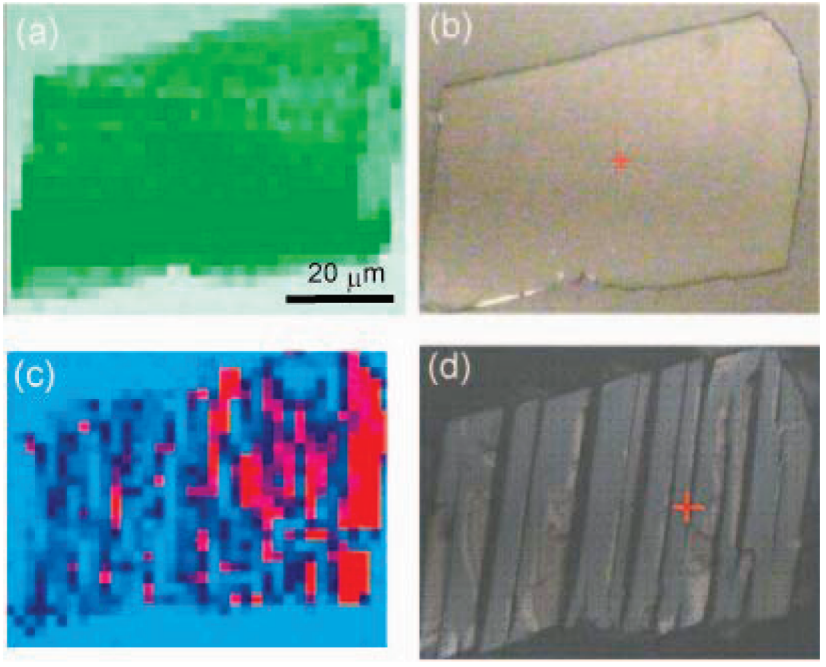

Figure 2. Raman and optical images of a large crystal. (a) Raman map and (b) optical image of the blue form, (c) Raman map and (d) optical image of the red/blue forms.

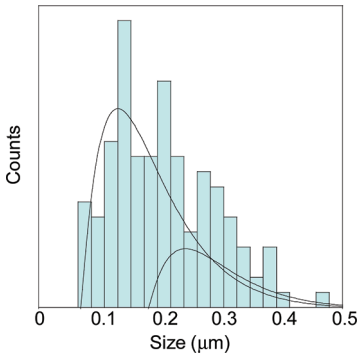

Figure 3. Size distribution of PCDA nanocrystals. Two curves are drawn to indicate the primary particles and their aggregates.

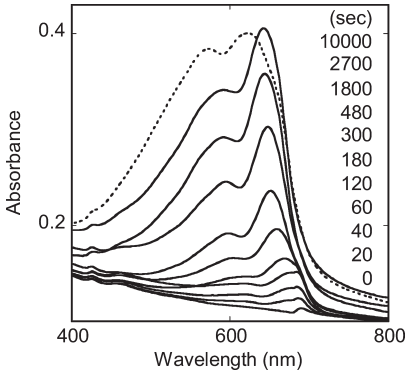

Figure 4. UV−vis absorption spectra of the PCDA nanocrystals in PS under UV irradiation for each indicated duration at 20 °C.

implies the average nanocrystal separation of 0.3 μm. Simplifying the CRM focus volume to be a cylinder, a pixel in Raman maps contains a sum of spectra from about 300 nanocrystals. As we shall show later, spatial inhomogeneity of nanocrystal distribution in PS occurs over around 20 μm. Therefore, the size and distribution of nanocrystals in the PS film can be taken as a continuum for CRM mapping, but is discrete for polymerization reaction.

3.4. Polymerization of Nanocrystals in PS. Figure 4 shows the time development of UV−visible (UV−vis) absorption spectra as the nanocrystals in PS were polymerized at 20 °C by irradiation of UV light. Initially, a small peak appears at 690 nm. It grows and blue-shifts toward 650 nm as the blue form polymer is synthesized. It takes over 5000 s before the red form becomes dominant. These spectral characteristics are identical to Langmuir−Blodgett multilayers of PCDA.[13] A similar spectral change was observed by polymerization at −24 and 3 °C. At 60 °C, however, the sample had already acquired a blue color during thermal equilibration before UV irradiation.

The absorbances at the maximum wavelength around 650−690 nm at 20 and −24 °C are summarized in Figure 5, respectively. At low conversion, since only the blue form is present, the absorbance is proportional to the polymer concentration. As the blue form is transformed into the red, the absorbance at the maximum wavelength appears to decrease, and the proportionality is lost. At 20 °C, the absorption increases linearly until 400 s, indicating a constant velocity. After 400 s, the velocity slows down. At −24 °C, the linear regime is over by 200 s, after which the absorbance approaches continuously to a

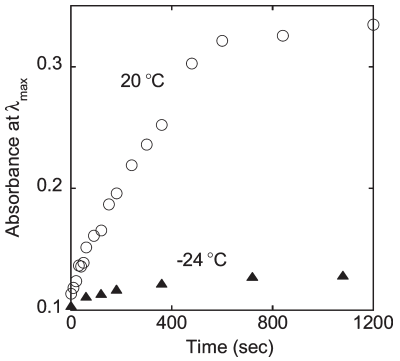

Figure 5. Time development of the polymerization of PCDA nanocrystals in PS at different temperatures, indicated as the maximum absorbance corresponding mostly to the blue form polymer in UV−vis absorption spectra.

constant value until 2000 s. Then, it starts increasing again and continues to increase even after 10 000 s (not shown). At both temperatures, the absorbance after the linear regime does not have a simple relation with the polymer concentrations due to the contributions from both the color transition and the saturated conversion. Both curves indicate the absence of autocatalytic polymerization, as commonly seen in aromatic diacetylene derivatives.[14,15] There is a report suggesting that autocatalysis is suppressed as a crystal size gets small.[16] In this study, we focus on the linear regime at very short irradiations. It is clear that the *average* polymer concentration over a centimeter scale increases linearly and faster at higher temperature.

3.5. Raman Mapping of Nanocrystals Polymerized at Various Temperatures. Unlike large crystals, the monomer nanocrystals produced sufficient Raman intensities for mapping. Figure 6 exhibits Raman maps of the monomer nanocrystals and the blue form polymer after irradiating UV light for 10 s at different temperatures, respectively. At each temperature, mapping was made at the same fixed location in PS films. The Raman intensity variation of each species within a scanned area is around 20−30% and is binarized to produce a Raman map, in order to make the comparison easier. A dark region corresponds to the *low* monomer intensity, but is inverted to mean the *high* polymer intensity. Instability during solvent evaporation has caused inhomogeneous distribution of the monomer nanocrystals over around 20 μm scale. At −24 °C, the dark areas of monomer and polymer maps are inverted, meaning that the high monomer intensity region gives the high polymer intensity region. On the other hand, at 20 °C, the monomer and polymer maps appear very similar, indicating that the low monomer intensity region becomes the high polymer intensity region. At 3 °C, while some areas show a high monomer-to-high polymer conversion, other areas exhibit the reversed situation. These results are reproducible over different locations of several independently prepared samples and are not caused by optical artifacts.

3.6. Crystalline Structures. All PCDA monomer nanocrystals were formed by solvent evaporation at room temperature. Then they were brought to the designated temperature for polymerization. If the monomer crystallized into multiple modifications, topochemical polymerization may give varying results depending on the lattice parameters of each structure. Although XRD is a powerful technique for structural determination, it is faced with the problem that X-rays polymerize PCDA monomer at room temperature. As for WAXRD, it has the additional difficulty of the

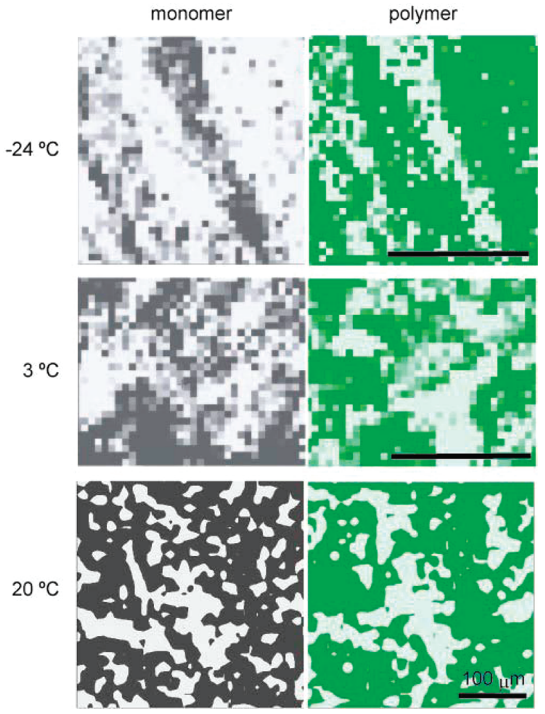

Figure 6. Raman maps of the binarized intensities of the monomer and the blue form polymer at various temperatures, respectively. For monomer, a dark region corresponds to high intensity. For polymer, a dark region refers to low intensity.

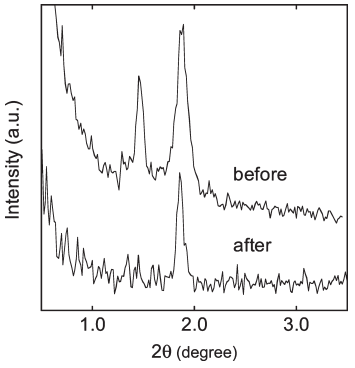

Figure 7. SAXRD spectra of the nanocrystal in PS before and after a short UV irradiation.

broad PS amorphous peak obscuring the monomer peaks around 4−5 Å.

Figure 7 shows SAXRD spectra of the nanocrystal in PS film before and after a short UV irradiation. Before the irradiation, two peaks are observed at 48 and 60 Å. After the irradiation, the peak at 60 Å disappears, and only the 48 Å peak remains. WXARD spectra also exhibit higher order peaks of these periods. A previous study of Langmuir−Blodgett films of Cd salt of PCDA gave a diminishing period at 54.4 Å and a growing period at 46.5 Å in the course of polymerization.[17] A polymerized crystal of Na salt of PCDA gave a single period at 55.2 Å.[18] PCDA forms a head-to-head bilayer structure by intermolecular hydrogen bonding between carboxylic acids. Since the observed periods are shorter than the extended length of two molecules (68.6 Å), these results have been explained by a model where straight monomeric units are tilted with respect to the bilayer plane with varying angles. The presence of a polymer peak in the monomer sample indicates that some monomer has polymerized during measurement. Since only a single period is detected for each monomer and polymer, respectively, the nanocrystals consist of only one kind of crystalline modification.

3.7. Thermal Properties of PCDA Nanocrystals in PS. DSC of PCDA monomer nanocrystals in PS measured from −30 to 80 °C yields a flat curve with a single sharp endothermic peak at 61.3 °C, the melting point of PCDA monomer. Within instrumental error, there are indications of neither thermal polymerization nor any thermal transitions occurring between −24 and 20 °C.

3.8. Spatial Variations of Nanocrystal Polymerization at Different Temperatures. In the present case, the Raman intensity of a given functional group depends on the absorbance, the electronic structure, and the concentration. The excitation wavelength of 780 nm is located at the diminishing tail of the absorption peak given in Figure 4 so that blue-shifting of the absorption maximum does not significantly affect the Raman intensity at low conversion. Since there is only a single kind of crystalline structure in each monomer and blue form polymer, the Raman intensity directly reflects the amount of each species. Therefore, the result of CRM mapping implies that, at −24 °C, the higher monomer concentration yields more polymers, which agrees with the well-known reaction kinetics of radical polymerization in macroscopic systems. In contrast, at 20 °C, the higher monomer concentration gives fewer polymers than the lower monomer concentration. This is a completely opposing result to common reactions and requires an explanation. It should be noteded that all monomer nanocrystals were prepared under the same conditions (at the same time as a single batch), and only the temperature of polymerization reaction differed. Furthermore, all samples were UV-irradiated for very short periods, i.e., close to the low conversion limit.

The present experimental conditions of unpolarized UV light and irradiation from random directions exclude the possibility of position-dependent photoinitiation, which is conceivable by the fact that each nanocrystal is optically anisotropic[19] and they are likely to be oriented locally in PS. The same conditions also ensure that the number of UV photons per unit volume remains constant over the entire area. Thus, photoinitiation occurs equally in each nanocrystal, which leads to the common observation that the higher monomer concentration yields more polymers.

The concentration of monomer is determined by the size and number density of nanocrystals. Under the present condition of low conversion, there are only a few initiation points in each nanocrystal. A previous study of γ-ray polymerization of an aromatic diacetylene has shown that the molecular weight of polymer remains small at low conversion.[20] These observations suggest that the probability of different propagating chains meeting each other within the same nanocrystal is small, regardless of the crystal size. For nanocrystals, a propagating chain has a higher probability of encountering one of the crystal surfaces than other chains. Once one of the diradials at the growing end reaches the crystal surface, it may be terminated or chain-transferred to a different monomer belonging to the next nanocrystal. In other words, the only way the number density affects the photoinitiated reaction is that it is so high as to make a significant number of nanocrystals in direct contact realize chain-transfer. Since a monomer is crystallized into nanocrystals under a constant initial amount,

the presence of such a high nanocrystal concentration region necessarily produced a region of extremely low nanocrystal concentration. The experimentally observed intensity variation of 20−30% does not support such a difference. Thus, most propagating chains reaching the surface are likely to be terminated. In this case, the maximum polymer length is affected by the crystal size. Since this effect is based on geometry only, it does not explain the observed temperature difference. The topochemical polymerization is also terminated by monomer lattice dislocations whose density may depend on the crystal size. The dislocations, however, were created during the formation of nanocrystals and should have affected the polymerization at all temperatures equally.

In macroscopic systems, most aliphatic diacetylenes do not polymerize thermally except at very high temperatures.[21−23] The present nanocrystals, however, acquired a blue color without UV irradiation at 60 °C. As for our DSC measurement, considering a small amount of PCDA (0.14 mg) in PS film and usually a very broad exothermic peak of thermal polymerization, it is possible that DSC failed to detect minute thermal polymerization. As long as polydiacetylene is concerned, optical properties are much more sensitive to reaction than thermal ones because only a small number of acetylene bonds suffice for the color change. These considerations suggest that polymerization can be initiated thermally in the nanocrystals at much lower temperatures. Since the average conversion over the cm^3 scale is higher at 20 °C than −24 °C, the result of CRM mapping can be interpreted as the low monomer region at 20 °C has polymerized more than the amount extrapolated from −24 °C, rather than the polymerization has been depressed at the high monomer region. As discussed above, the continuous supply of an equal number of photons to each nanocrystal leads to a high-monomer-to-high-polymer relation. We propose that thermal initiation is responsible for the inverted relation, yielding more polymers at the low monomer region. PS has one of the lowest thermal conductivities (around 0.1 W/mK) among polymers. Once thermal energy is lost by initiation, it is not easily compensated from outside at low conversion. With a limited amount of energy available for thermal initiation, more energy is allocated to each nanocrystal in the low monomer region than ones in the high region. At −24 °C, photoinitiation dominates. At 20 °C, in addition to photoinitiation, thermal initiation becomes significant, enhancing polymerization of nanocrystals in the low monomer region. At 3 °C, thermal initiation is not so strong, giving mixed regions of different types.

The thermal initiation also explains why the present difference was observed in the dispersed nanocrystals but not in the large crystal. As mentioned above, aliphatic diacetylenes are resistant to thermal initiation compared with aromatic ones. Then, the crystal surface should play an important role for aliphatic compounds since the molecules at the surface are expected to have the largest thermal energy. Having a large fraction of surfaces, nanocrystals should be more susceptible to thermal initiation than the large crystal. Additionally, it is generally observed that solid crystals have higher thermal conductivity than amorphous forms. Thermal energy can be transferred more evenly within a large crystal than among the dispersed nanocrystals in PS.

3.9. Transition Scales for Proper Averaging. In the case of a large crystal, photopolymerization to the blue form appears to proceed uniformly; that is, spatial averaging has been established within a scale smaller than the mapping resolution of 2 μm. This makes sense since photoinitiation is a monomeric event that occurs randomly at many places in the submicrometer scale. On the other hand, the color transition to the red form was discernible with each broken piece of about 5 μm. The color transition originates from the crystalline stress, which requires the lattice strain accumulated over several micrometers for PCDA. We need to take an average over the whole crystal if we are to discuss quantities such as the degree of the color transition.

As for nanocrystals in PS at low conversion, about 20 μm is the transition scale above which averaging fades out polymerization inhomogeneity. If our proposal based on the thermal initiation property of the monomer and thermal conductivity of the matrix is correct, this scale should depend on the choice of monomer and matrix materials. In the present case, a volume of 20 × 20 × 10 μm^3 contains about 10^5 nanocrystals, which may be taken as the minimum number of nanocrystals necessary to make a correspondence between macroscopic measurements such as UV−vis absorption spectroscopy and microscopic measurements.

4. CONCLUSIONS

The scale at which spatial averaging yields a meaningful value is shown to be determined by the process governing the reaction. Photoinitiation in the large crystal is a monomeric event and requires a scale much smaller than the CRM resolution, whereas the color transition originates from crystalline stress and needs averaging over the whole crystal. Thermal initiation in the dispersed nanocrystals is limited by thermal conductivity of the matrix, and the transitional averaging scale in the present case is over 20 μm. Because nanocrystals are usually embedded in liquid or solid matrices, it is important to realize that not only the properties of the nanocrystal but also those of the surroundings have significant influence on the proper averaging scales.

The present study is based on CRM observation, which limits the spatial resolution to approximately 0.5 μm even under better conditions. Processes such as photoinitiation and chain transfer in both macroscopic and nano systems have already been averaged at this scale. In nano systems, however, the occurrences of some of these processes become rare *per crystal*. A study of temporal averaging may be possible even with the CRM spatial resolution.

AUTHOR INFORMATION

Corresponding Author

*E-mail address: mass@yz.yamagata-u.ac.jp.

REFERENCES

(1) Flory, P. J. *Principles of Polymer Chemistry*; Cornell University Press: London, 1953; Chapter 13.
(2) Enkelmann, V. *Adv. Polym. Sci.* **1984**, *63*, 91–134.
(3) Sixl, H. *Adv. Polym. Sci.* **1984**, *63*, 50–90.
(4) Mino, N.; Tamura, H.; Ogawa, K. *Langmuir* **1991**, *7*, 2336–2341.
(5) Carpick, R. W.; Mayer, T. M.; Sasaki, D. Y.; Burns, A. R. *Langmuir* **2000**, *16*, 4639–4647.
(6) Everall, N. J. *Appl. Spectrosc.* **2000**, *54*, 773–782.
(7) Kamath, M.; Kim, W. H.; Li, L.; Kumar, J.; Tripathy, S.; Babu, K. N.; Talwar, S. S. *Macromolecules* **1993**, *26*, 5954–5958.
(8) Batchelder, D. N.; Evans, S. D.; Freeman, T. L.; Håussling, L.; Ringsdorf, H.; Wolf, H. *J. Am. Chem. Soc.* **1994**, *116*, 1050–1053.
(9) Saito, A.; Urai, Y.; Itoh, K. *Langmuir* **1996**, *12*, 3938–3944.
(10) Itoh, K.; Nishizawa, T.; Yamagata, J.; Fujii, M.; Osaka, N.; Kudryashov, I. *J. Phys. Chem. B* **2005**, *109*, 264–270.
(11) Seto, K.; Hosoi, Y.; Furukawa, Y. *Chem. Phys. Lett.* **2007**, *444*, 328–332.

(12) Bloor, D.; Kennedy, R. J.; Batchelder, D. N. *J. Polym. Sci. Polym. Phys. Ed.* **1979**, *17*, 1355–1366.
(13) Tieke, B.; Lieser, G.; Wegner, G. *J. Polym. Sci. Polym. Chem. Ed.* **1979**, *17*, 1631–1644.
(14) Chance, R. R.; Patel, G. N. *J. Polym. Sci. Polym. Phys. Ed.* **1978**, *16*, 859–881.
(15) Baughman, R. H. *J. Chem. Phys.* **1978**, *68*, 3110–3121.
(16) Gerasimov, G. N.; Stanislavskii, Y. S.; Kir'yanova, T. V.; Eremicheva, Y. N.; Teleshov, E. N.; Trakhtenberg, L. I. *Polym. Sci. B* **2001**, *43*, 54–57.
(17) Shufang, Y.; Huilin, Z.; Pingsheng, H. *J. Mater. Sci.* **1999**, *34*, 3149–3154.
(18) Pang, J.; Yang, L.; McCaughey, B. F.; Peng, H.; Ashbaugh, H. S.; Brinker, C. J.; Lu, Y. *J. Phys. Chem. B* **2006**, *110*, 7221–7225.
(19) Volkov, V. V.; Asahi, T.; Masuhara, H.; Masuhara, A.; Kasai, H.; Oikawa, H.; Nakanishi, H. *J. Phys. Chem. B* **2004**, *108*, 7674–7680.
(20) Wenz, G.; Wegner, G. *Mol. Cryst. Liq. Cryst.* **1983**, *96*, 99–108.
(21) Tieke, B.; Bloor, D.; Young, R. J. *J. Mater. Sci.* **1982**, *17*, 1156–1166.
(22) Laxhuber, L. A.; Scheunemann, U.; Möhwald, H. *Chem. Phys. Lett.* **1986**, *124*, 561–566.
(23) Shibasaki, Y.; Fukuda, K.; Nishimoto, Y. *J. Therm. Anal.* **1993**, *40*, 491–497.